J|A|C|S COMMUNICATIONS

Published on Web 02/18/2010

Nanocrystal Growth on Graphene with Various Degrees of Oxidation

Hailiang Wang, Joshua Tucker Robinson, Georgi Diankov, and Hongjie Dai*

Department of Chemistry and Laboratory for Advanced Materials, Stanford University, Stanford, California 94305

Received January 13, 2010; E-mail: hdai@stanford.edu

As a single-atom-thick carbon material with light weight and high surface area and conductivity, graphene[1,2] could be an ideal substrate for growing and anchoring of functional nanomaterials for high-performance electrocatalytic or electrochemical devices. Nanocrystals grown on graphene could have an enhanced electron transport rate, high electrolyte contact area, and structural stability, all of which could be useful for various fundamental and practical applications.[3] Although decoration of nanoparticles on graphite oxide (GO) sheets has been shown,[4−6] it remains unexplored and highly desirable to synthesize nanocrystals on more pristine graphene with high electrical conductivity, control the morphologies of the nanocrystals by tuning the degree of oxidation of the graphene sheets, and rationalize the nanocrystal growth behavior.

Here we show a general two-step method for growing hydroxide and oxide nanocrystals of the iron family elements (Ni, Co, Fe) on graphene with two degrees of oxidation. Drastically different nanocrystal growth behaviors were observed on low-oxidation graphene sheets (GS) and highly oxidized GO in hydrothermal reactions. Small particles precoated on GS with few oxygen-containing surface groups diffused and recrystallized into single-crystalline nanoplates or nanorods with well-defined shapes. In contrast, particles precoated on GO were pinned by the high-concentration oxygen groups and defects on GO without recrystallization into well-defined morphologies. Our results suggest an interesting approach for controlling the morphology of nanocrystals by tuning the surface chemistry of graphene substrates used for crystal nucleation and growth.

Our GS with a low degree of oxidation were made by an exfoliation−reintercalation−expansion method,[7−9] and GO was produced by a modified Hummers method[10] (Figure 1). The resistivity of our GS was measured to be only several times higher than that of pristine graphene but ∼100 times lower than that of GO in reduced form.[7−9] The oxygen content in the GS (∼5%) was much lower than in GO (∼20%), as measured by Auger spectroscopy[9] and X-ray photoelectron spectroscopy (XPS).[11]

In the first step of $Ni(OH)_2$ growth on graphene, we deposited precursor materials in the form of small nanoparticles uniformly nucleated onto GS or GO by hydrolysis of $Ni(CH_3COO)_2$ at 80 °C in a 10:1 *N*,*N*-dimethylformamide (DMF)/water mixture (see the Supporting Information). The 10:1 DMF/H_2O ratio was found to be important to afford good dispersion of graphene and a low rate of hydrolysis that led to selective and uniform coating of nickel hydroxide on graphene, with little particle growth in the free solution. After the first step, dense and uniform $Ni(OH)_2 \cdot 0.75H_2O$ nanoparticles (10−20 nm in diameter) were formed on both GS and GO, as revealed by scanning electron microscopy (SEM) (Figures 2a and 3a) and X-ray diffraction (XRD) (Figure S1a,b in the Supporting Information). The mass percent of $Ni(OH)_2 \cdot 0.75H_2O$ was ∼87% in the graphene composite. As a control, when water was used as the sole solvent, we observed appreciable $Ni(OH)_2 \cdot 0.75H_2O$ particle growth in the free solution instead of on GS as a result of fast hydrolysis.

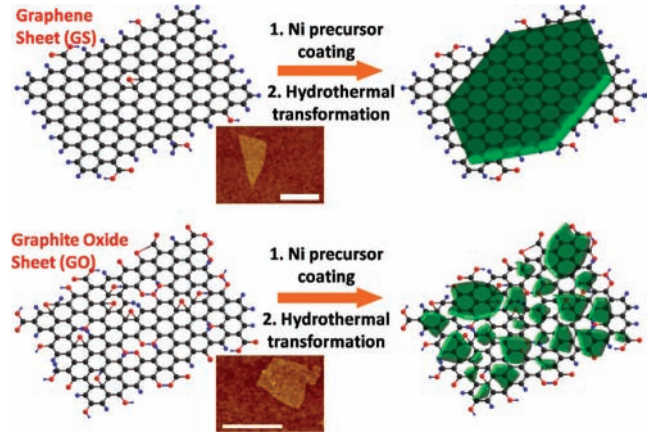

Figure 1. Schematic illustration of two-step $Ni(OH)_2$ nanocrystal growth on (top) graphene sheets (GS) and (bottom) graphite oxide (GO). Dark gray balls, C atoms; blue balls, H atoms; red balls, O atoms; green plates, $Ni(OH)_2$. Insets: AFM images of GS and GO. Scale bars: 500 nm. After the first step of the growth process (Ni precursor coating), the same coating of $Ni(OH)_2 \cdot 0.75H_2O$ was obtained both on GS and GO. After the second step (hydrothermal transformation), however, the coating on GS diffused and recrystallized into large single-crystalline hexagonal $Ni(OH)_2$ nanoplates, while the coating on GO remained as densely packed nanoparticles pinned by the functional groups and defects on the GO surface.

In the second step, we hydrothermally treated the product of the first step, i.e., $Ni(OH)_2 \cdot 0.75H_2O$ coated GS at 180 °C in water (see the Supporting Information). We observed that the coating material evolved from dense small particles into hexagonal nanoplates selectively attached to GS (Figure 1 top panel and Figure 2b,c). The side length of the nanoplates was several hundred nanometers, and their thickness was ≲10 nm (Figure 2b,c and Figure S2). XRD of a thick layer of packed nanoplates on GS suggested crystalline β-$Ni(OH)_2$ formed on graphene (Figure 2d). High-resolution transmission electron microscopy (HRTEM) (Figure S3) clearly revealed the (100) and (010) lattice fringes in the plane of a single-crystalline hexagonal $Ni(OH)_2$ nanoplate on GS. The corresponding fast Fourier transform (Figure S3 inset) of the HRTEM image was consistent with a hexagonal lattice perpendicular to the (001) zone axis, suggesting $Ni(OH)_2$ nanoplates attached to GS at their (001) planes. In a film of the packed $Ni(OH)_2$/GS plates for XRD experiments, a large fraction of the plates were packed parallel to each other and the substrate, giving an enhanced (001) diffraction peak in the XRD spectrum (Figure 2d). Scanning Auger electron spectroscopy (SAES) elemental imaging of Ni and C elements in the $Ni(OH)_2$/GS composite further confirmed attachment of $Ni(OH)_2$ nanoplates on GS (Figure S4).

The same $Ni(OH)_2 \cdot 0.75H_2O$ coating obtained on GO was transformed into small nanoparticles of β-$Ni(OH)_2$ densely packed on GO (forming a continuous film) after the second step of hydrothermal treatment at 180 °C (Figure 1 lower panel and Figure 3) without production of large single-crystalline hexagonal nanoplates as in the GS case. These results showed that the size,

10.1021/ja100329d

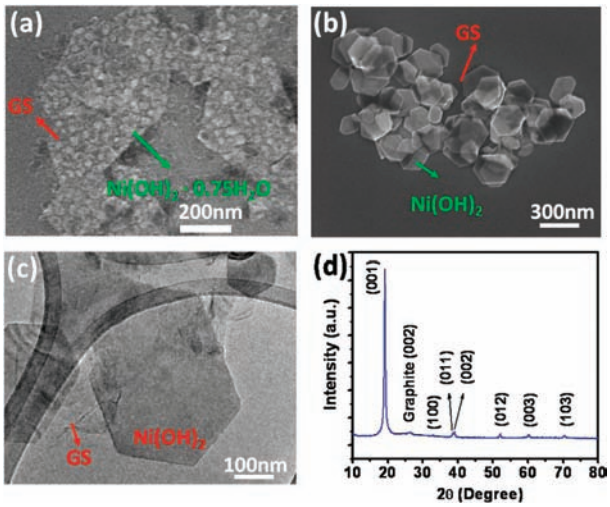

Figure 2. (a) SEM image of $Ni(OH)_2 \cdot 0.75H_2O$ particles uniformly coated on GS after the first step of growth at 80 °C. (b) SEM image of $Ni(OH)_2$/GS after the second step of simple hydrothermal treatment of the product depicted in (a) at 180 °C. (c) TEM image of hexagonal $Ni(OH)_2$ nanoplates formed on top of GS. (d) XRD spectrum of a packed thick film of hexagonal $Ni(OH)_2$ nanoplates on GS.

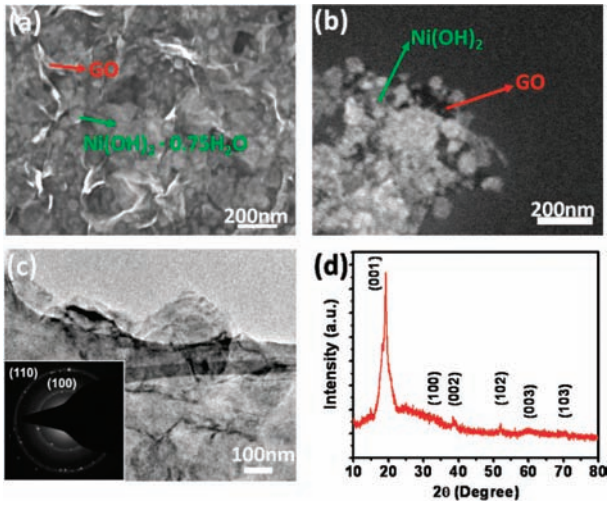

Figure 3. (a) SEM image of $Ni(OH)_2 \cdot 0.75H_2O$/GO after the first step of growth at 80 °C. (b) SEM image of $Ni(OH)_2$/GO after the second step of growth at 180 °C. (c) TEM image of $Ni(OH)_2$/GO spanning the holes on a TEM grid. Inset: electron diffraction pattern of $Ni(OH)_2$ on GO. (d) XRD spectrum of a packed thick film of $Ni(OH)_2$ nanoparticles on GO.

morphology, and crystallinity of the nanocrystals formed on graphene are dependent on the degree of oxidation of the underlying graphene substrate. We suggest that GS with fewer functional groups and defects exhibit weaker chemical interactions with coating species on the surface. During the 180 °C hydrothermal reaction, the small coating particles on GS diffused across the "slippery" graphitic lattice and recrystallized into single-crystalline hexagonal nanoplates on the GS. On GO, however, because of the higher density of oxygen functional groups, including carboxylic, hydroxyl, and epoxy groups,[7,9−12] the GO surface interacts strongly with the coated species, providing pinning forces to the small particles to hinder diffusion and recrystallization. As a result, most of the $Ni(OH)_2 \cdot 0.75H_2O$ particles coated on GO by the first growth step remained pinned at their original positions after the second step of hydrothermal treatment at higher temperature. In the case of $Ni(OH)_2$/GS, it is plausible that both chemisorption and van der Waals interactions between $Ni(OH)_2$ nanoplates and graphene exist, at oxygen-containing defect sites and pristine regions of the GS, respectively.

We found this two-step synthesis on graphene with different degrees of oxidation to be a general approach for controlling nanocrystal morphology (Figures S5−S8). By controlling the reaction temperature in the second step, we produced CoO(OH) and Fe_2O_3 nanocrystals with regular nanoplate and nanorod morphologies on GS, using $Co(CH_3COO)_2$ and $Fe(CH_3COO)_2$ as precursors (Figures S5c and S7c), respectively. On GO, only small, irregularly shaped nanoparticles resulted (Figures S5f and S7f). These results confirm that graphene with various degrees of oxidation can be used as a novel substrate for the growth of nanocrystals into various sizes and morphologies. Adjusting the second-step reaction temperature can be included to further control the materials grown on graphene. For particles with weak interactions with graphene, increasing the reaction temperature eventually led to diffusion and recrystallization of surface species into larger crystals on GO (Figure S9).

In summary, we have developed a two-step method for growing nanocrystals with well-defined nanoplate or nanorod morphologies on weakly interacting and highly conducting graphene surfaces. The morphology of the nanocrystals formed on graphene can be tailored by the degree of oxidation of graphene and the reaction temperature, and the method could be extended to synthesize a wide range of functional nanomaterials.

Acknowledgment. This work was supported in part by ONR.

Supporting Information Available: Experimental details about making GS and GO and about nanocrystal growth of $Ni(OH)_2$, CoO(OH), and Fe_2O_3 on GS and GO; additional SEM, TEM, XRD, and SAES characterizations of nanocrystal/graphene composites. This material is available free of charge via the Internet at http://pubs.acs.org.

References

(1) Geim, A. K.; Novoselov, K. S. *Nat. Mater.* **2007**, *6*, 183–191.
(2) Li, X.; Wang, X.; Zhang, L.; Lee, S.; Dai, H. *Science* **2008**, *319*, 1229–1232.
(3) Simon, P.; Gogotsi, Y. *Nat. Mater.* **2008**, *7*, 845–854.
(4) Williams, G.; Seger, B.; Kamat, P. V. *ACS Nano* **2008**, *2*, 1487–1491.
(5) Si, Y.; Samulski, E. T. *Chem. Mater.* **2008**, *20*, 6792–6797.
(6) Yang, X.; Zhang, X.; Ma, Y.; Huang, Y.; Wang, Y.; Chen, Y. *J. Mater. Chem.* **2009**, *19*, 2710–2714.
(7) Li, X.; Zhang, G.; Bai, X.; Sun, X.; Wang, X.; Wang, E.; Dai, H. *Nat. Nanotechnol.* **2008**, *3*, 538–542.
(8) Wang, H.; Wang, X.; Li, X.; Dai, H. *Nano Res.* **2009**, *2*, 336–342.
(9) Wang, H.; Robinson, J. T.; Li, X.; Dai, H. *J. Am. Chem. Soc.* **2009**, *131*, 9910–9911.
(10) Sun, X.; Liu, Z.; Welsher, K.; Robinson, J. T.; Goodwin, A.; Zaric, S.; Dai, H. *Nano Res.* **2008**, *1*, 203–212.
(11) Li, X.; Wang, H.; Robinson, J. T.; Sanchez, H.; Diankov, G.; Dai, H. *J. Am. Chem. Soc.* **2009**, *131*, 15939–15944.
(12) Mkhoyan, K. A.; Contryman, A. W.; Silcox, J.; Stewart, D. A.; Eda, G.; Matteyi, C.; Miller, S.; Chhowalla, M. *Nano Lett.* **2009**, *9*, 1058–1063.

JA100329D